45th AIAA Aerospace Sciences Meeting and Exhibit
8 - 11 January 2007, Reno, Nevada

AIAA 2007-662

The Low Reynolds Number Aerodynamics of Leading Edge Flaps

N.M. Bakhtian* and H. Babinsky†
Department of Engineering, University of Cambridge, Trumpington St., Cambridge, CB2 1PZ, England

A.L.R. Thomas‡ and G.K. Taylor§
Department of Zoology, University of Oxford, South Parks Road, Oxford, OX1 3PS, England

Within the low Reynolds number regime at which birds and small air vehicles operate (Re=15,000-500,000), flow is beset with laminar separation bubbles and bubble burst which can lead to loss of lift and early onset of stall. Recent video footage of an eagle's wings in flight reveals an inconspicuous wing feature: the sudden deployment of a row of feathers from the lower surface of the wing to create a leading edge flap. An understanding of the aerodynamic function of this flap has been developed through a series of low speed wind tunnel tests performed on an Eppler E423 aerofoil. Experiments took place at Reynolds numbers ranging from 40000 to 140000 and angles of attack up to 30º. In the lower range of tested Reynolds numbers, application of the flap was found to substantially enhance aerofoil performance by augmenting the lift and limiting the drag at certain incidences. The leading edge flap was determined to act as a transition device at low Reynolds numbers, preventing the formation of separation bubbles and consequently decreasing the speed at which stall occurs during landing and manoeuvring.

Nomenclature

C_D : drag coefficient
C_L : lift coefficient
$C_{L,max}$: maximum lift coefficient
R : approximate flow reattachment point
Re : chord Reynolds number
S : approximate flow separation point
α : angle of attack
ΔC_L : change in lift coefficient

I. Introduction

Low Reynolds number flows, the regime in which birds and MAVs operate, are characterized by their propensity to induce transitional separation bubbles on the airfoil surface. This complex boundary layer phenomenon resulting from the implications of laminar flow and involving flow separation, transition, and reattachment has been studied in depth[1-3]. The size and position of separation bubbles are determined by factors

*Research Student, Aerodynamics Laboratory, Department of Engineering, University of Cambridge, Student Member AIAA
†Reader in Aerodynamics, Department of Engineering, University of Cambridge, Senior Member AIAA
‡Professor of Biomechanics, Department of Zoology, University of Oxford, Member AIAA
§Royal Society University Research Fellow, Department of Zoology, University of Oxford, Member AIAA

including the Reynolds number, severity and location of the adverse pressure gradient, freestream turbulence level, and surface roughness[3]. Short bubbles, typically covering only a few percent of the chord, are generally defined to have little effect on the overall pressure distribution and hence the performance of the airfoil, while long bubbles, covering up to 40% of the airfoil surface, are recognized to have a significant negative impact. Long separation bubbles radically impair the pressure distribution, smearing the peak and generating an immense loss of lift and increase in drag, by changing the effective airfoil shape about which the freestream flows[1]. With changing conditions, separation bubbles can evolve into completely separated flow over the surface, resulting in so-called bubble burst[1,2,4,5] and leading edge stall.

The adverse effects of separation bubbles and bubble burst which dominate at low Reynolds numbers can be overcome by various means. Transition control, in particular, involves the enhancement of airfoil performance by either advancing transition or by attempting to maintain laminar flow and suppress flow separation and bubble effects. A thorough discussion of accepted flow control methods is presented by Gad-el-Hak[2]. The former idea, the act of tripping the flow, is based on the idea that separation bubbles may be prevented altogether if the laminar flow transitions into turbulent flow upstream of the laminar separation point[6]. The most anticipative method of altering the transition behavior of an airfoil is to originally design it (leading edge curvature, camber and thickness) such that the severity of the adverse pressure gradient leads to transition at the desired location[2]. Barring that, the most direct method of ensuring transition is to introduce a turbulence trip[1,2] (typically a roughened surface or simple two-dimensional trip) into the flow. Lissaman[1] also mentions the use of fixed wires or grids in the airflow ahead of the model which accelerate transition by increasing the freestream turbulence. In experiments involving a 1mm wire placed a distance of 10% chord in front of the leading edge, Schmitz[7] describes a significant delay in stall as compared to the clean airfoil at the same Reynolds numbers. It has recently been recognized that short leading edge separation bubbles, themselves, can be exploited as transition control devices[1,8,9]. Experimental smoke flow visualizations and lift measurements performed by Mueller and Batill[3] demonstrate a shift in flow behavior from large-scale separation to mostly attached flow with increasing incidence due to formation of a leading edge separation bubble. This enhanced performance is caused by the flow transition in the bubble's shear layer which

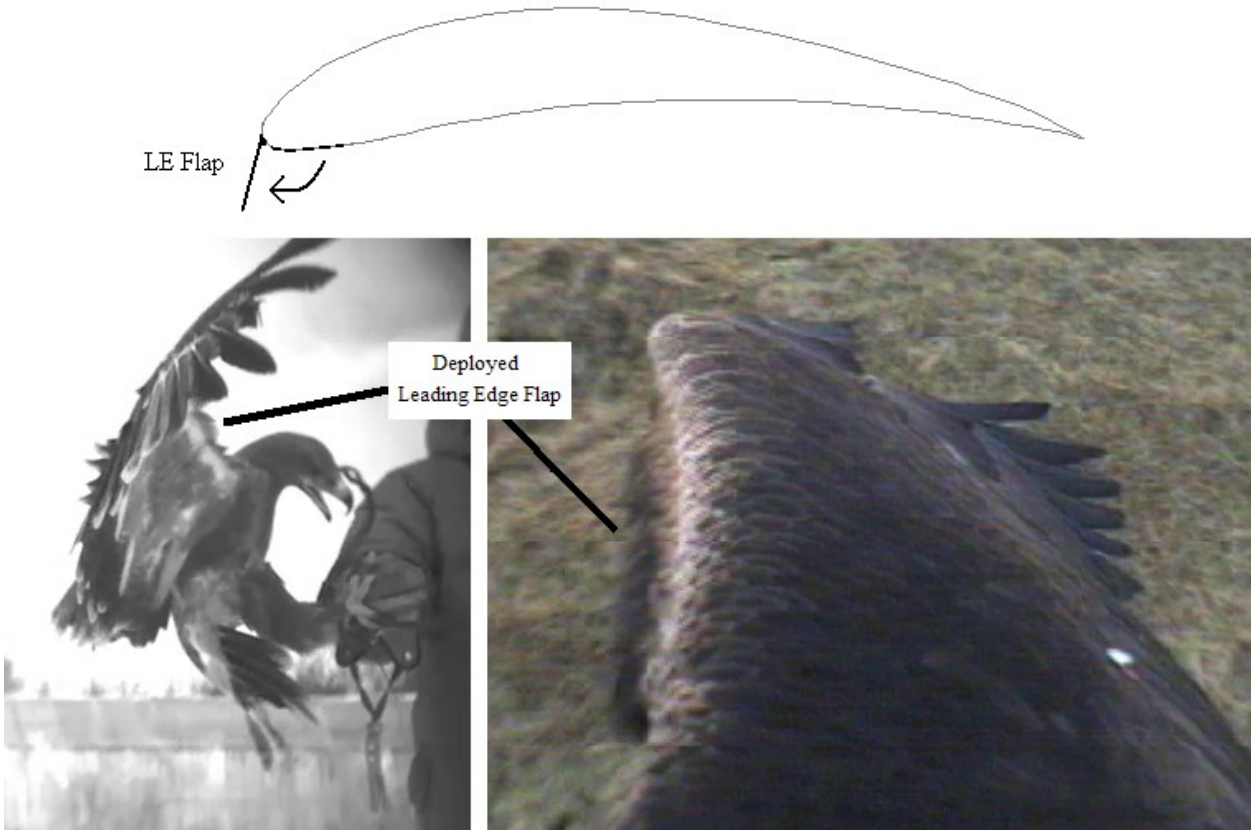

Figure 1: Deployed flap as seen on eagle wing

then precludes laminar separation over the remainder of the airfoil. Lissaman[1] notes that a careful balance must be maintained for each of these transition-inducing mechanisms; in order to provoke turbulence, they must be of significant magnitude, but over-designed trips lead to unnecessarily thick boundary layers which result in higher drag and an advancement of trailing edge separation.

Further solutions to the negative effects imposed by laminar flows can be found in nature, which provides an example of myriad "biological flying machines" evolved over millions of years to master low Reynolds number flight[10]. Observations of birds in flight have led to the discovery of numerous auxiliary devices including split wings[11], alulae[11,12], and upper surface self-activated flaps[13,14], parallels to which can be found in modern aircraft.

A further, thus far unresearched, feature found on certain birds' wings is a row of feathers at the anterior region, a leading edge flap of sorts, which is seen to deploy intermittently in flight as illustrated in Figure 1. This phenomenon, briefly mentioned by Hertel[11] and Azuma[12] as a high-lift device, has more recently been subject to analysis by Carruthers et al.[15] by means of high speed video footage. Observations of eagles in flight have shown that the feathers "pop out" during landing and certain manoeuvres.

The intent of this research is to explore the possibility of this leading edge flap acting as a high lift device. Experimental work presented by Fullmer[16], in which a similar Kruger-like flap was deployed from the lower surface of the airfoil, shows a 30% increase in maximum lift coefficient at $Re=6x10^{6.}$ The Kruger flap[17-19], along with the droop nose (nose flap)[19,20] and slat[19,21], is a mechanical high lift device used in high Reynolds number powered flight. Such leading edge devices typically work to alleviate the severe pressure gradient and thus act to extend the lift curve by delaying leading edge stall[22]. However, their utility in low Reynolds number flows, the regime in which the observed avian flap is found to operate, has not been well documented and might well be inadequate due to the differing flow characteristics over the range of Reynolds numbers.

The focus of the present work is to experimentally establish the aerodynamic function of the observed leading edge flap at low Reynolds numbers and to propose a mechanism by which application of the flap realizes any improvements to the lift and drag characteristics of the baseline aerofoil. In addition to providing increased insight on the science of low Reynolds number flow and bird flight, this research has the potential to lead to the implementation of this possible high lift flow control device on micro air vehicles and unmanned aerial vehicles (MAV/UAV), whose flight also falls into the low Reynolds number range.

II. Experimental Setup

A. Experimental Apparatus

Experiments have been performed in the 1A low speed wind tunnel (Figure 2) of the Engineering Department at the University of Cambridge. The open-return tunnel, capable of speeds up to 25m/s, has a rectangular working section measuring 0.715m in width and 0.510m in height. Turbulence intensity was measured using a hot-wire anemometry system and found to be approximately 0.10% between 10m/s to 20m/s. Below this range, only slightly higher turbulence intensity values were measured.

Chosen for its highly cambered profile, an Eppler E423 airfoil with a chord length of 97.25mm has been used in all experiments. The aluminum model, with an aspect ratio of just over 7.3, spans close to the entire width of the tunnel. Full-span, stainless steel flaps (Figure 2) were rigidly fastened to the leading edge of the airfoil using five tin plate attachment brackets. A plastic film covering along the entire span on the upper surface ensured an airtight seal between the airfoil and flap.

Lift and drag force measurements were taken with the use of an externally-mounted, 2-component 50N strain gauge balance shown in Figure 2. Force balance measurements were supplemented with rough data on separation and reattachment points from surface oil flow visualization utilizing a mixture of kerosene, titanium dioxide and oleic acid.

B. Experimental Parameters

Each airfoil configuration was tested over a range of Reynolds numbers (Re) and angles of attack (α). A baseline Reynolds number, using the chord as the reference length, was calculated as 95000 assuming an eagle wing chord of 30cm and a maximum landing speed of 5m/s[23]. The tested range comprised Reynolds numbers of 40000, 70000, 95000, 120000, and 140000. Tunnel speed was noted through use of a standard pitot-static tube positioned upstream of the model measuring the freestream dynamic pressure.

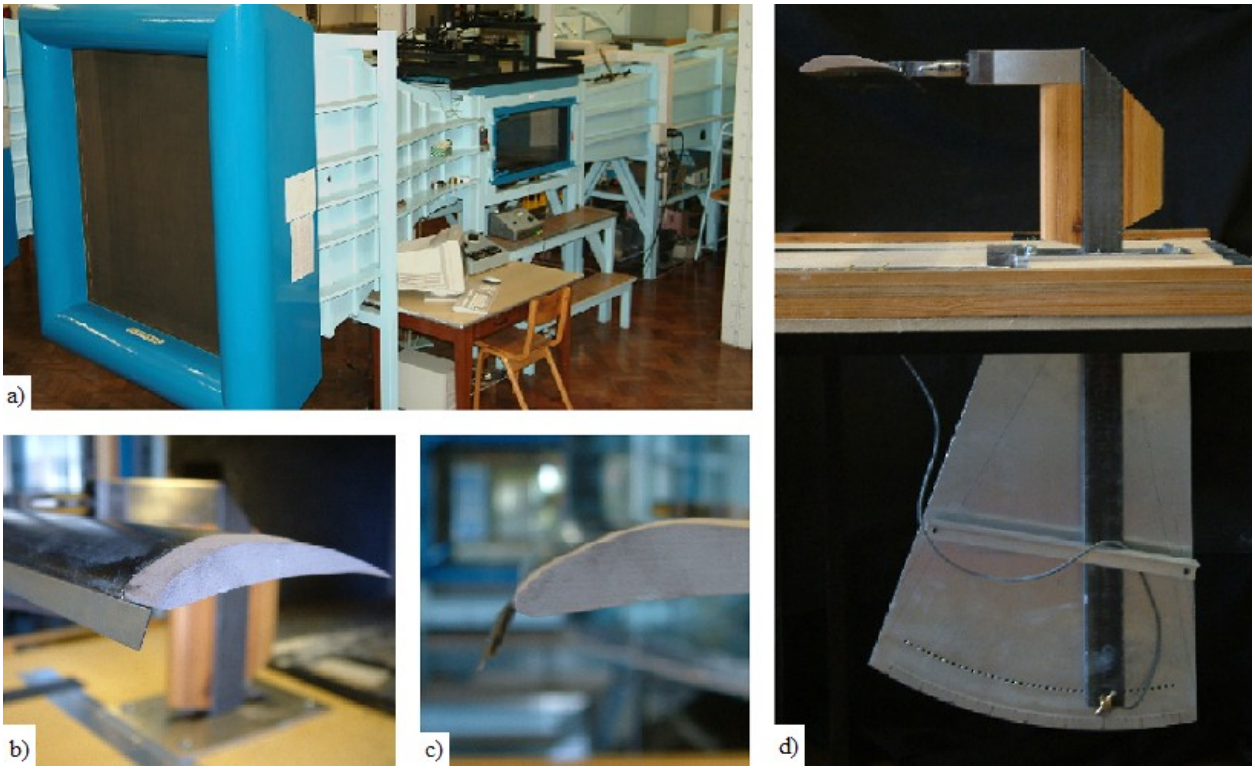

Figure 2: Experimental arrangement. a) 1A low speed tunnel, b) and c) airfoil with a leading edge flap, and d) force balance set-up- airfoil and sting balance mounted to the tunnel floor

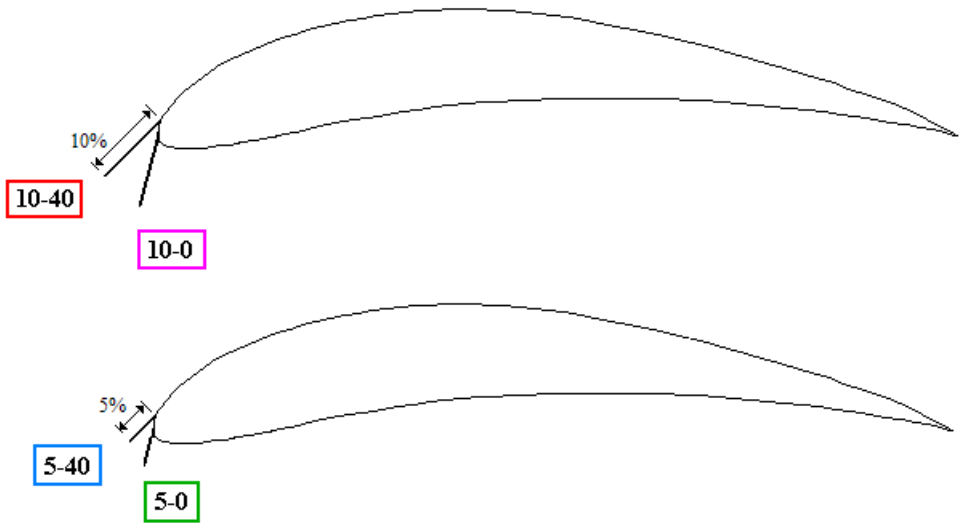

Figure 3: Four flap configurations tested on an Eppler E423 airfoil

The basic leading edge flap characteristics of length and deployed position were varied in experiment, as exact quantitative data from live birds has yet to be taken. Flap lengths of 5mm and 10mm, corresponding to approximately 5% and 10% of chord length, respectively, were each tested in two fixed deployed positions. The hinge point and orientation are described by Bakhtian[24]. Henceforth, the four tested flap configurations will be referred to by the names indicated in Figure 3. The increase in chord due to addition of the flaps was taken into account in the lift and drag coefficient calculations. Recorded angles of attack, however, remained defined with respect to the baseline airfoil chord line[20].

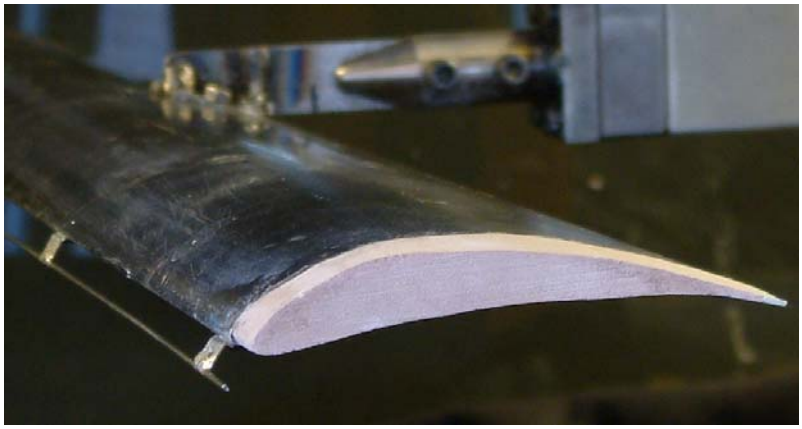

Figure 4: Wire trip configuration

In addition to the four flap configurations, two types of transitional device were tested on the baseline airfoil: a tape trip on the upper surface of the airfoil and a wire trip located forward of the leading edge of the airfoil. The tape trip consisted of a 0.12mm thick, 19mm wide piece of smooth electrical tape spanning the entire airfoil. The leading edge of this trip was placed at approximately 5% chord. The second transition device, portrayed in Figure 4, was a wire trip comprised of a rigid cylindrical wire with diameter 1.1mm spanning the entire airfoil and held in place by five attachment brackets. In contrast to the tape trip, the wire trip was placed in the freestream flow upstream of the leading edge, specifically positioned in the same location as the leading edge of the 5-40 flap.

C. Experimental Uncertainty and Corrections

Uncertainties were calculated using a standard error propagation technique. The uncertainty in angle of attack is of the order of 0.4º. Error in flap length and position could range up to 0.2mm, 5% in hinge position, and 10% in orientation position. The error in Reynolds number, including both systematic and random errors, is approximately 4% for the median Reynolds number case, Re=95000. Uncertainties in the calculations for C_L and C_D lead to approximate errors of 7% for the median Reynolds number case. The low Reynolds number tests, however, are found to carry a 23% error. With respect to the oil flow visualization results, the separation line can only be accurately noted to within 5% of the chord length. The error in point of reattachment, being more difficult to identify, increases to 10% of the chord length..

Wind tunnel boundary corrections were calculated using the methods put forth by Pope and Harper[25]. Calculations of the solid two-dimensional blocking factor, wake blocking, and correction for streamline curvature lead to the following: an effective C_L ranging from 0.92 and 0.98 and an effective C_D ranging from 0.93 to 0.99 of the uncorrected values. The correction factors described are minimal and fall close to the uncertainty range for C_L and C_D. Uncertainty and corrections are not indicated on the drag polars for the sake of clarity. More importantly, the main focus here is not to establish definite quantitative values but to examine changes in flow behavior.

III. Results and Discussion

Force results are presented in the form of drag polar plots. Most tests were run between 0º and 30º angle of attack in 1º increments; those which began to experience vibrations during testing were consequently tested to lower incidences. Seven different cases or testing configurations are alluded to: baseline airfoil, the four flap cases (10-40, 10-0, 5-40, and 5-0), tape trip, and wire trip.

Images of oil flow patterns over the airfoil upper surface provide a visual confirmation of the flow dynamics at specific Reynolds numbers and angles of attack. These oil test points (OTPs) are labeled individually on the corresponding polar plots. Separation (S) and reattachment (R) points were recorded during oil flow testing- if flow lines exist in the photographs downstream of the marked S position or upstream of the marked R position, these resulted from flow effects experienced during the spin-up or spin-down of the tunnel fan (flow at a lower Re). Flow is from left to right in all images.

A. Baseline Airfoil

The drag polar plotted in Figure 5 shows baseline airfoil data (no flap) at a range of Reynolds numbers including lower Re (40000 and 70000), intermediate Re (95000 and 120000), and higher Re (140000). The Re=140000 curve, with steadily increasing lift and a C_L of over 2.0 at 14º, indicates a relatively healthy attached flow. The remainder of the curves show a rapid decrease in lift production as the angle of attack increases, resulting in lift coefficients limited to around C_L=1.3. This drastic change in performance is typical of low Reynolds number flows. The low lift, high drag Re=40000, 70000, and 95000 curves are indicative of the separated flow over the majority of the aerofoil's upper surface, or separation bubble burst. OTP-A,B (Figure 6) show the upstream progression of the separation point from approximately 30% to 10% of the chord, measured from the leading edge, with no subsequent reattachment as α increases from 4º to 19º. This significant separation over the upper surface occurs even at low incidences and leads to early stall for the Reynolds numbers below 140000.

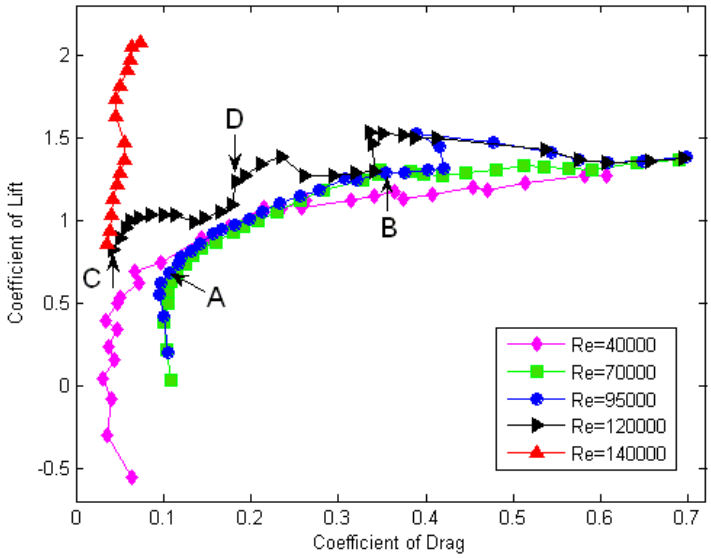

Figure 5: Baseline airfoil polars at various Reynolds numbers

On closer inspection, the Re=120000 curve and, to some extent, the Re=95000 curve show some variation from the poor performance just described. At certain angles of attack, the flow for these two cases seems to somewhat recover as the lift coefficient increases from approximately C_L=1.3 to C_L=1.5. OTP-C,D (Figure 6) show the upstream progression of a separation bubble at Re=120000 as the angle of attack is increased. Overall, the baseline results indicate that the lift and drag characteristics of the aerofoil are far from ideal in a range of attack angles and Reynolds numbers.

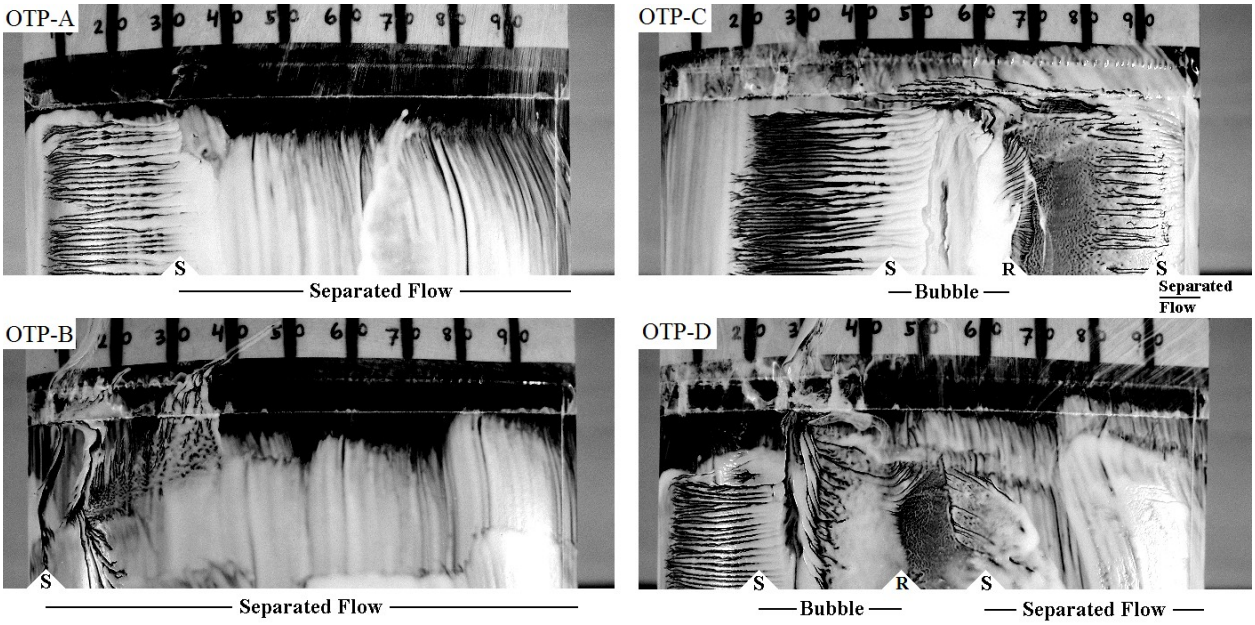

Figure 6: [OTP-A] Baseline airfoil, Re=95000, α=4º [OTP-C] Baseline airfoil, Re=120000, α=0º
[OTP-B] Baseline airfoil, Re=95000, α=19º [OTP-D] Baseline airfoil, Re=120000, α=12º

B. Airfoil with Flaps

Drag polars of the performance of the four flap configurations as compared to the baseline airfoil are shown in Figure 7. It can clearly be seen that the flow experiences a drastic change in performance due to application of the leading edge flap. However, this occurs only at certain incidences. At a Reynolds number of 40000 at low angles of attack (0º-10º), addition of leading edge flap to the airfoil results only in a much higher drag than experienced by the baseline airfoil. Up until an incidence of 21º, the lift characteristics for the flap configurations remain similar to the baseline case, experiencing the slow decrease in lift slope gradient characteristic of advancing separation. At this α of 21º, the 5-40 flap configuration first deviates from the low-lift curve and seems to reach a new lift level at an incidence of about 24º. The addition of the flap results in a lift coefficient of 1.65 at this α which is an increase of 0.52 (46%) over the baseline configuration. The 10-40 flap also is shown to experience this cross-over to a different flow behavior, but at a higher incidence of 27º.

At Reynolds numbers of 70000 and 95000, all four flap configurations are seen to exhibit the same improvement, a rapid increase in lift and drop in drag, to an even greater extent than in the Re=40000 cases. Flap-induced maximum lift coefficients range up to $C_{L,max}$=1.82 (10-45 flap, 26º at Re=95000). Oil flow visualization demonstrates that the high lift shown in the flap cases corresponds to a delay in separation, or an increase in the amount of attached flow over the airfoil upper surface as compared to the baseline configuration. OTP-E,F (Figure 8) illustrate the flow behaviors of the baseline and 5-40 flap configurations at Re=70000 and α=19º. The flap has augmented the amount of attached flow over the upper surface almost three-fold, leading to an increase in C_L of 0.31 as compared to the baseline airfoil at the same α. Similarly, OTP-B,H (Figure 8) show the increase in attached flow seen with addition of the 5-40 flap at Re=95000 and α=19º. Analogous patterns in the drag polar curves are seen at a Reynolds number of 120000 although model vibrations prevented high-α testing in all configurations.

Figure 7 shows a trend in the performance of the flap configurations. Above a certain threshold angle of attack which varies depending on configuration, the flap is able to ameliorate the poor flow characteristics at all tested Reynolds numbers (Re=40000-120000) through a jump in lift and decrease in drag. At lower angles of attack, all flap cases remain in the unhealthy, separated flow state similar to that of the baseline airfoil.

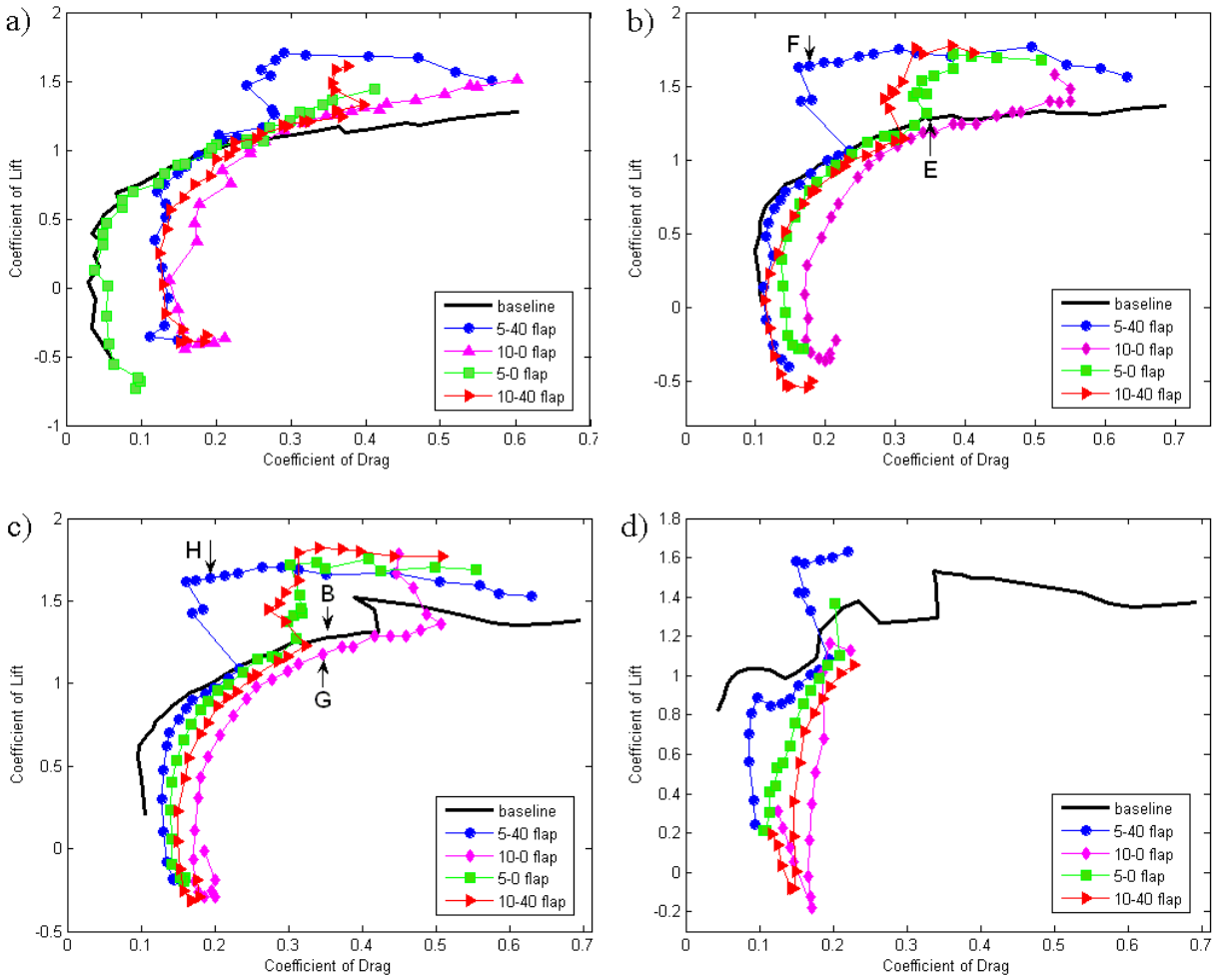

Figure 7: Flap configuration polars as compared to baseline polar at a) Re=40000, b) Re=70000, c) Re=95000 and d) Re=120000

C. Airfoil with Transition Trips

In order to clarify the mechanism by which the flap induces this effect, several transition trip devices were tested. Figure 9 shows drag polars comparing the tape trip and wire trip configurations with the baseline and 5-40 flap configurations. At the lower Reynolds numbers, Re=40000 and 70000, the tape trip has no effect on the low lift, high drag baseline airfoil performance, whereas the wire trip is shown to improve the flow characteristics in the same manner as the leading edge flap. At the higher tested Reynolds numbers, Re=95000 and 120000, both trip configurations improve the baseline airfoil flow but in a seemingly different manner, as suggested by the dissimilar curve shapes.

At high Re (Re=95000 and Re=120000), the tape trip is able to dramatically improve the baseline airfoil flow at low and intermediate angles of attack ($\alpha<26^{o}$), with lift coefficients reaching almost 2.0. Oil flow visualisation confirms that this is achieved through an increase in attached flow, manifested in OTP-A,L and OTP-B,H,M in Figure 8. A comparison at Re=95000 and $\alpha=19^{o}$ (OTP-B,H,M) shows flow separation at 70% chord in the tape trip configuration- an improvement over the separation points at 5% and 20% in the baseline and flap configurations, respectively. OTP-L shows reattachment of the flow after separation, resulting in a separation bubble at Re=95000 and $\alpha=4^{o}$ in contrast to the baseline case (OTP-A) in which the flow fails to reattach.

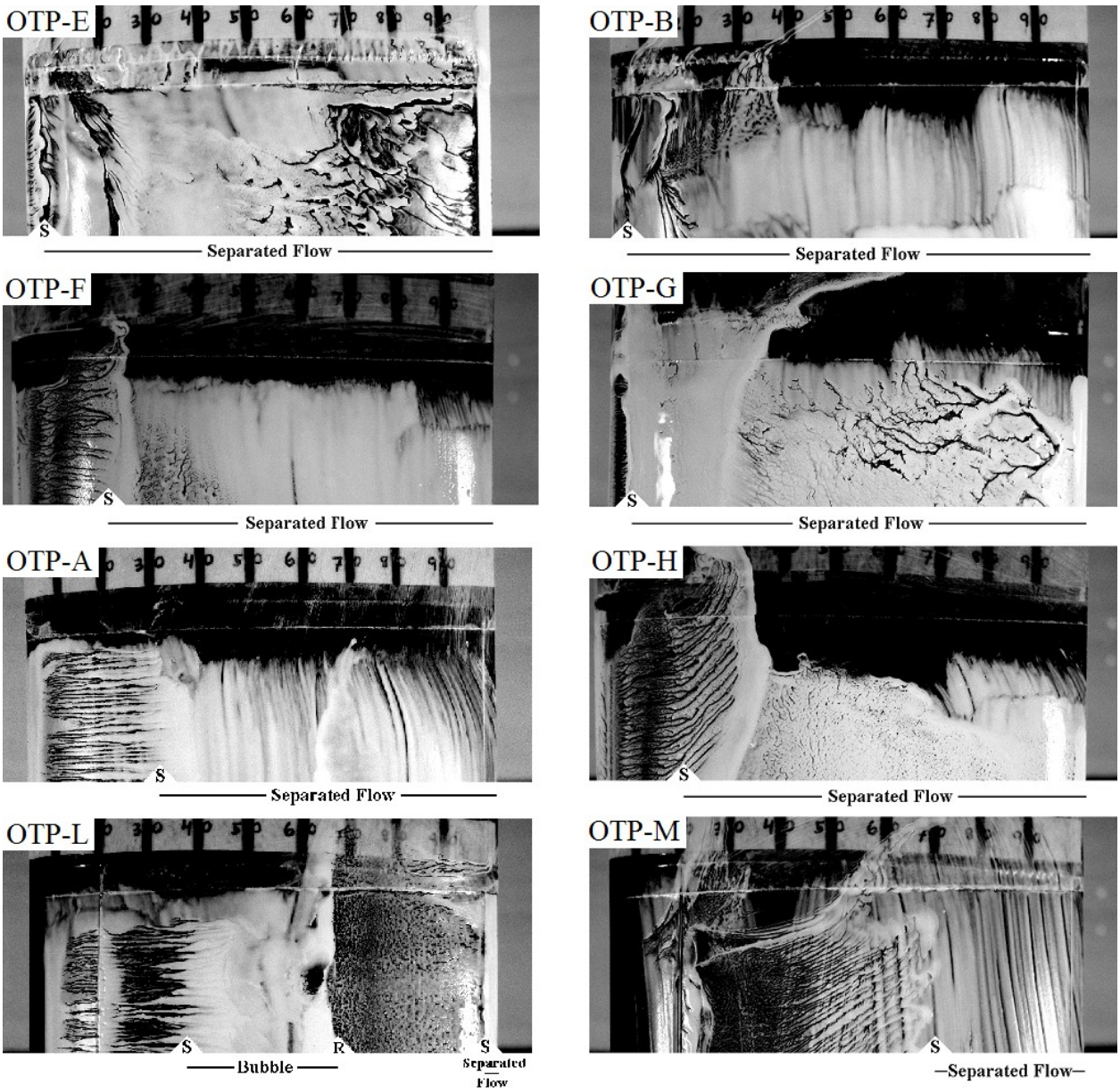

Figure 8: [OTP-E] Baseline, Re=70000, α=19º
[OTP-F] 5-40 flap, Re=70000, α=19º
[OTP-A] Baseline, Re=95000, α=4º
[OTP-L] Tape trip, Re=95000, α=4º
[OTP-B] Baseline, Re=95000, α=19º
[OTP-G] 10-0 flap, Re=95000, α=19º
[OTP-H] 5-40 flap, Re=95000, α=19º
[OTP-M] Tape trip, Re=95000, α=19º

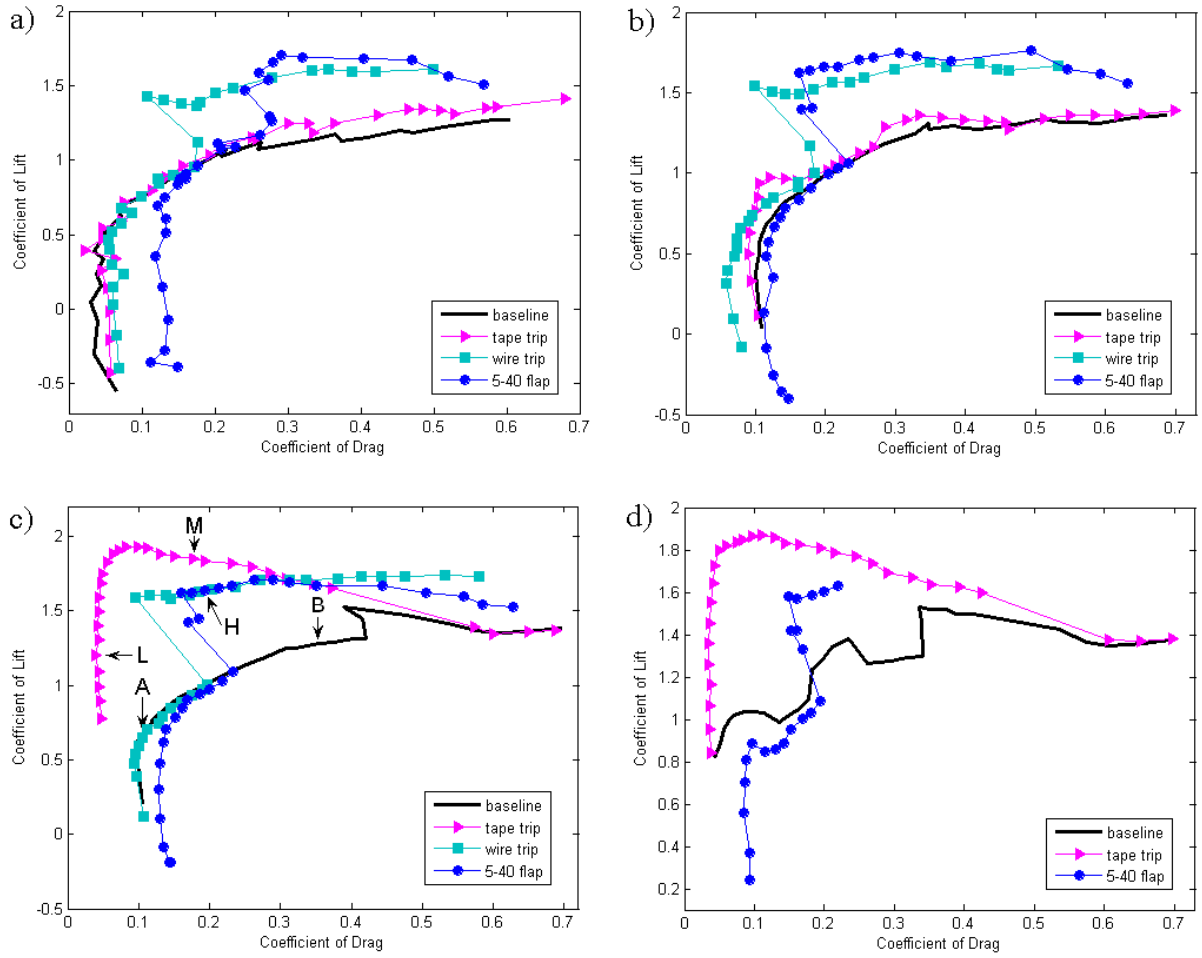

Figure 9: Wire and tape trip configuration polars as compared to the baseline and 5-40 flap polars at a) Re=40000, b) Re=70000, c) Re=95000 and d) Re=120000

Low attack angles, producing weaker pressure peaks, allow laminar flow which inevitably leads to an upper surface laminar separation over the baseline airfoil and, in the case of low Reynolds numbers, bubble burst (OTP-A). However, the disturbances from the surface step change (tape trip), allowed to propagate by the intermediate and higher Reynolds numbers, are thought to cause a rapid transition to turbulence in the separated shear layer leading to reattachment and formation of a separation bubble rather than total bubble burst (OTP-L). At higher angles of attack, the strengthened leading edge pressure peak combined with instabilities caused by the trip allow turbulent flow to develop even nearer the leading edge. Lift begins to taper off as turbulent trailing edge separation point moves toward the leading edge, visualized in OTP-M. These flow effects occur even without the surface trip, but only at the highest Reynolds numbers (Re=140000), as seen in Figure 5.

Thus, as shown, the tape trip provides for higher lift at only the intermediate Reynolds numbers. At low Reynolds numbers, the tape trip is unable to effect a positive change in the airfoil's performance, and at Re=140000, the baseline airfoil already experiences good flow quality.

Although the airfoil does benefit from addition of the tape trip at intermediate Reynolds numbers, its drag polar curve is dissimilar to the curve corresponding to the leading edge flap effect. In the flap case, a sudden jump in lift and drop in drag takes place over a few angles of incidence, while in the tape trip case, lift and drag develop smoothly over the entire α range.

In contrast, examination of the flow behavior resulting from the application of a wire trip illuminates a remarkable similarity between the drag polar curves of the wire trip and flap configurations. The wire trip exhibits the same jump at similar incidences at each tested Reynolds number (not tested at Re=120000). This sudden change in behavior is thought to be a consequence of the wire's position upstream of the leading edge. As seen in Figure 10, any disturbances created by the wire trip do not pass over the upper surface leading edge at low incidences, thus inhibiting its ability to trip the flow. Once the airfoil's angle of attack has increased sufficiently, the instabilities formed in the wake of the wire trip engulf the upper leading edge of the airfoil and trip the transition to turbulent flow. With this introduction of a turbulent boundary layer, laminar separation is no longer possible and the lift and drag are observed to change.

As seen in Figure 9, at Re=95000 the wire trip and flap cases don't reach the same $C_{L,max}$ as the tape trip configuration. It is thought that the tripwire and flap, resulting in a faster transition on the upper surface of the airfoil due to their anterior positioning as compared to the tape trip, would experience an earlier trailing edge separation thus causing a milder increase in lift. Of particular note is the wire trip's ability to improve the flow even at the lowest Reynolds numbers at which the tape trip did not. It is possible that the separation bubble caused by the flap introduces a stronger disturbance into the boundary layer that follows which is not stabilized as easily.

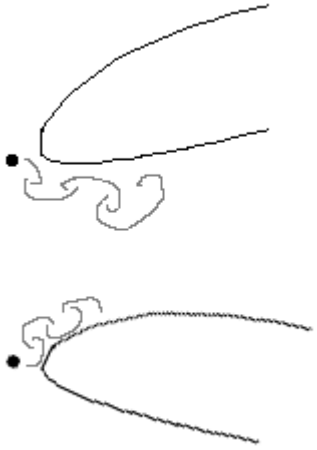

Figure 10: Effect of wire trip at 0º and 30º angle of attack

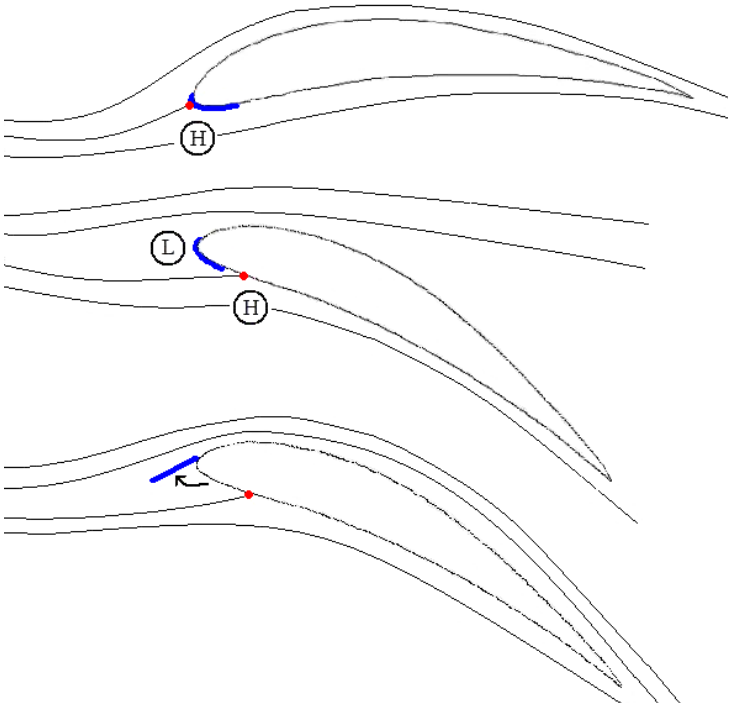

Figure 11: Flap deployment mechanism

D. Flap Mechanism

The comparable flow characteristics as inferred by the drag polars suggest that a similar mechanism must be responsible for the effects of both the wire trip and the leading edge flap.

As in the case of the trip wire, the flap has minimal effect at low incidences due to its misalignment with the oncoming flow. Once a certain intermediate angle of attack is reached, ranging from 13º to 24º depending on the Reynolds number, the flow is able to navigate the sharp leading edge presented by the flap and passes over the flap upper surface and onto the airfoil upper surface. It is believed that at increasing angles of attack, a miniature separation bubble is formed on the leading edge of the flap terminating in laminar reattachment, as the Reynolds number is too small at that point to foster a turbulent transition. This separation and subsequent reattachment incite disturbances in the flow over the remaining portion of the flap which pass on to the upper surface of the airfoil and behave in the same manner as the wake disturbances produced by the trip wire. A second possibility is that the

disturbances in the flow produced by the sharp leading edge of the flap cause an early separation on the airfoil. These disturbances could be strong enough to quickly trip the transition to turbulent flow and consequently lead to the formation of a small transitional separation bubble. In short, disturbances created upstream of the leading edge flow over the upper surface of the airfoil, causing a premature transition to turbulence and thus preventing the formation of detrimental laminar separation bubbles. The flap acts as a transition device.

As the flap has been observed only during certain regimes of avian flight (landing, take-off, and certain manoeuvres), a mechanism by which the flap deploys and re-stows must exist whether it be by passive or active means. High speed video footage (500 frames per second) of the flap deploying during landing reveals the time it takes to fully deploy is on the order of 100ms[15]. Deployment is thus believed to take place passively and not through active muscle use. A possible passive mechanism is shown in Figure 11. As the angle of attack is increased, the stagnation point moves from the leading edge onto the lower surface of the wing. Once the stagnation point has moved beyond the leading edge of the stowed flap, the low pressure in the region covering the light feathers which compose the flap will cause the flap to rapidly deploy.

Re-examining the drag polars (Figure 7) resulting from experimental application of the leading edge flap in a rigidly deployed position, the flap clearly only has a positive effect once a certain limiting angle of attack is achieved. At incidences below that, the experimental flap serves only to increase the drag as the flow separates behind the flap. At these low incidences, the flap as found on a bird would not be deployed because the stagnation point would fall onto the flap itself. It is believed, then, that the flap found in nature deploys at those angles of attack at which it may function properly and positively impact the flow dynamics.

IV. Conclusions

Observations of birds, naturally-evolved low Reynolds number fliers, have led to the discovery of a row of feathers at the wing leading edge of certain species which intermittently deploys from the lower surface. This work describes and interprets experimental wind tunnel data obtained on the aerodynamic function of this leading edge flap at low Reynolds numbers. Fixed-flap testing showed distinct performance enhancement at Reynolds numbers of 40000-120000 and angles of attack greater than 20º, a regime in which the baseline airfoil experienced detrimental laminar separation effects. The tested flaps were found to increase the baseline airfoil's lift coefficient by up to ΔC_L=0.52.

It is surmised that the leading edge flap acts, not as a high-lift device in the traditional sense, but as a transition device, precluding the customary low Reynolds number afflictions of laminar separation bubbles and bubble burst over the remainder of the lifting surface. This conclusion results from the striking similarity between the sudden jump in lift observed in the flap configuration and that due to the applied transition wire mounted forward of the airfoil at the position of the flap leading edge.

A conventional boundary layer trip placed directly on the airfoil surface was found capable of incredible lift enhancement at higher Reynolds numbers, surpassing even the beneficial effects of the trip wire. However, the surface trip was unable to trip the flow below Re=95000 in contrast to the leading edge flap which was able to maintain the elevated lift curve at even these lower Reynolds numbers. Even more importantly, leading edge flaps are deployable and thus can be employed solely in off-design (high lift, low Re) flight functions such as landing and maneuvering without spoiling performance at the design point where flow tripping is unnecessary and usually detrimental. Furthermore, as it is believed that the flap experiences a passive deployment mechanism in avian flight, leading edge flaps have the potential for automatic deployment if implemented in man-made applications such as MAVs.

Acknowledgments

We would especially like to thank the Aerolab technicians- D. Martin, B. Stock, J. Hazlewood, and J. Clark- for their unfailing technical expertise and support. Thanks are also due to L. Crandal and Cossack for repeated flight maneuvers and landings despite wintry conditions. Finally, this research would not have been possible without the financial support of the Winston Churchill Foundation.

References

[1]Lissaman, P.B.S. (1983). Low-Reynolds-Number Airfoils. Annual Review of Fluid Mechanics. 15:223-239.

[2]Gad-el-Hak, M. (1990). Control of Low-Speed Airfoil Aerodynamics. AIAA Journal. 28:1537-1552.

[3]Mueller, T.J. and Batill, S.M. (1982). Experimental Studies of Separation on a Two-Dimensional Airfoil at Low Reynolds Numbers. AIAA Journal. 20:457-463.

[4]Roberts, W.B. (1980). Calculation of Laminar Separation Bubbles and Their Effect on Airfoil Performance. AIAA Journal. 18:25-31.

[5]Gaster, M. (1969). The Structure and Behaviour of Laminar Separation Bubbles. Aeronautical Research Council, R. & M. No. 3595.

[6]Häggmark, C. (2000). Investigations of Disturbances Developing in a Laminar Separation Bubble Flow. Technical Report, Royal Institute of Technology, Department of Mechanics, Stockholm, Sweden.

[7]Schmitz, F.W. (1983). Aerodynamik des Flugmodells. Luftfahrt-Verlag Axel Zuerl. Germany.

[8]Lutz, T., Würz, W. and Wagner, S. (2001). Numerical Optimization and Wind-Tunnel Testing of Low Reynolds Number Airfoils. In Fixed and Flapping Wing Aerodynamics for Micro Air Vehicle Applications, Mueller, T.J., editor. American Institute of Aeronautics and Astronautics.

[9]Lee, C.S., Pang, W.W., Srigrarom, S., Wang, D., and Hsiao, F. (2006). Classification of Airfoils by Abnormal Behavior of Lift Curves at Low Reynolds Numbers. AIAA 2006-3179.

[10]Pines, D.J. and Bohorquez, F. (2006). Challenges Facing Future Micro-Air-Vehicle Development. Journal of Aircraft. 43:290-305.

[11]Hertel, H. (1963). Structure, Form, Movement. Reinhold Publishing Corporation, New York.

[12]Azuma, A. (1992). The Biokinetics of Flying and Swimming. Springer-Verlag, Tokyo.

[13]Bechert, D.W., Bruse, M., Hage, W., and Meyer, R. (1997). Biological Surfaces and their Technological Application – Laboratory and Flight Experiments on Drag Reduction and Separation Control. Proceedings of the 28th AIAA Fluid Dynamics Conference, 4th AIAA Shear Flow Control Conference, June 29-July 2, 1997, Snowmass Village, Colorado.

[14]Schatz, M., Knacke, T., Thiele, F., Meyer, M, Hage, W., and Bechert, D.W. (2004). Separation Control by Self-Activated Movable Flaps. Proceedings of the 42nd AIAA Aerospace Sciences Meeting and Exhibit, January 5-8, Reno, Nevada.

[15]Carruthers, A.C., Taylor, G.K., Walker, S.M., and Thomas, A.L.R. (2007). Use and Function of a Leading Edge Flap on the Wings of Eagles. AIAA 2007-43.

[16]Fullmer, F.F. Jr. (1947). Two-Dimensional Wind-Tunnel Investigation of the NACA 64_1-012 Airfoil Equipped with Two Types of Leading-Edge Flap. NACA Technical Note No. 1277.

[17]Abbott, I.H. and Doenhoff, A.E. (1959). Theory of Wing Sections Including a Summary of Airfoil Data. Dover Publications, New York.

[18]Young, A.D. (1947). The Aerodynamic Characteristics of Flaps. Aeronautical Research Council. R. & M. No. 2622.

[19]Williams, A.L. (1986). A New and Less Complex Alternative to the Handley Page Slat. Journal of Aircraft. 23:200-206.

[20]Martin, P.B., McAlister, K.W., Chandrasekhara, M.S., and Geissler, W. (2003). Dynamic Stall Measurements and Computations for a VR-12 Airfoil with a Variable Droop Leading Edge. Presented at American Helicopter Society 59th Annual Forum, Phoenix, Arizona. May 6-8, 2003.

[21]Smith, A.M.O. (1975). High-Lift Aerodynamics. Journal of Aircraft. 12:501-530.

[22]Baragona, M., Boermans, L.M.M., van Tooren, M.J.L., Bijl, H., and Beukers, A. (2003). Bubble Bursting and Stall Hystersis on Single-Slotted Flap High-Lift Configuration. AIAA Journal. 41:1230-1237.

[23]Thomas, A.L.R. and Taylor, G.K. (2005). Department of Zoology, University of Oxford. Personal Communications.

[24]Bakhtian, N.M. (2006). The Low Reynolds Number Aerodynamics of Leading Edge Flaps. MPhil Thesis. University of Cambridge, UK.

[25]Pope, A. and Harper, J.J. (1966). Low-Speed Wind Tunnel Testing. John Wiley & Sons, Inc., New York.